ANTIOXIDANTS & REDOX SIGNALING
Volume 20, Number 17, 2014

DOI: 10.1089/ars.2013.5357

Therapeutics

FORUM ORIGINAL RESEARCH COMMUNICATION

NADPH Oxidase, NOX1, Mediates Vascular Injury in Ischemic Retinopathy

Jennifer L. Wilkinson-Berka,[1,2,*] Devy Deliyanti,[1,*] Indrajeetsinh Rana,[1] Antonia G. Miller,[1] Alex Agrotis,[1] Roksana Armani,[1] Cédric Szyndralewiez,[3] Kirstin Wingler,[4] Rhian M. Touyz,[5,6] Mark E. Cooper,[1,2] Karin A. Jandeleit-Dahm,[2,*] and Harald H.H.W. Schmidt[4,*]

Abstract

Aims: Ischemic retinal diseases such as retinopathy of prematurity are major causes of blindness due to damage to the retinal microvasculature. Despite this clinical situation, retinopathy of prematurity is mechanistically poorly understood. Therefore, effective preventative therapies are not available. However, hypoxic-induced increases in reactive oxygen species (ROS) have been suggested to be involved with NADPH oxidases (NOX), the only known dedicated enzymatic source of ROS. Our major aim was to determine the contribution of NOX isoforms (1, 2, and 4) to a rodent model of retinopathy of prematurity. ***Results:*** Using a genetic approach, we determined that only mice with a deletion of NOX1, but not NOX2 or NOX4, were protected from retinal neovascularization and vaso-obliteration, adhesion of leukocytes, microglial accumulation, and the increased generation of proangiogenic and proinflammatory factors and ROS. We complemented these studies by showing that the specific NOX inhibitor, GKT137831, reduced vasculopathy and ROS levels in retina. The source of NOX isoforms was evaluated in retinal vascular cells and neuro-glial elements. Microglia, the immune cells of the retina, expressed NOX1, 2, and 4 and responded to hypoxia with increased ROS formation, which was reduced by GKT137831. ***Innovation:*** Our studies are the first to identify the NOX1 isoform as having an important role in the pathogenesis of retinopathy of prematurity. ***Conclusions:*** Our findings suggest that strategies targeting NOX1 have the potential to be effective treatments for a range of ischemic retinopathies. *Antioxid. Redox Signal.* 20, 2726–2740.

Introduction

In ischemic retinopathies such as retinopathy of prematurity and diabetic retinopathy, tissue hypoxia is a predominant causative factor for the capillary degeneration and pathological neovascularization that characterize these diseases (45, 51). Retinopathy of prematurity is the major cause of vision loss and blindness in the neonate, a situation that is escalating in prevalence throughout the world (20, 60). Retinopathy of prematurity develops in some preterm infants following exposure to monitored hyperoxia, which disrupts physiological vascularization resulting in areas of vaso-obliteration (51). After subsequent maturation of the infant and return to room air, the nonvascularized retina becomes increasingly hypoxic. These changes in the retinal microenvironment stimulate the production of angiogenic factors, such as vascular endothelial growth factor (VEGF) and erythropoietin, resulting in pathological neovascularization (8, 45, 51). The vasculopathy that occurs in retinopathy of prematurity and diabetic retinopathy involves not only

[1]Department of Immunology, Monash University, Melbourne, Australia.
[2]JDRF Danielle Alberti Memorial Centre for Diabetic Complications, Baker IDI Heart and Diabetes Institute, Melbourne, Australia.
[3]Genkyotex, Geneva, Switzerland.
[4]Department of Pharmacology, CARIM, Maastricht University, Maastricht, The Netherlands.
[5]Institute of Cardiovascular and Medical Sciences, University of Glasgow, Glasgow, United Kingdom.
[6]Ottawa Hospital Research Institute, University of Ottawa, Ottawa, Canada.
*These authors contributed equally to this study.

Innovation

Our study provides novel insight into the role of particular NADPH oxidase (NOX) isoforms in the development of vascular injury, inflammation, and oxidative stress in ischemic retinopathy. Furthermore, the presence of NOX isoforms in retinal vascular and nonvascular cells suggests that particular cell populations drive reactive oxygen species (ROS)/NOX-mediated damage. We speculate that the inhibition of pathological NOX isoforms may provide a new avenue for the treatment of ischemic retinopathies, such as retinopathy of prematurity, where preventative mechanism-based therapies are urgently required.

vascular cells but also nonvascular cells (16). Indeed, inflammatory cells and the immune cells of the retina, microglia, play a critical role in the development and repair of the vasculature in retinopathy of prematurity (43, 50).

The treatment strategies for retinopathy of prematurity remain unsatisfactory. The main approach is the use of laser photocoagulation to decrease areas of damaged and hypoxic retina (31, 45). However, this treatment only provides benefits in the end stage of the condition, and unfortunately, neither prevents disease progression nor completely prevents vision loss. Therefore, new strategies that target the underlying mechanisms involved in the development of retinopathy of prematurity are urgently required (10, 12). A likely critical pathomechanism is an excessive generation of reactive oxygen species (ROS). The neonatal retina maintains a high rate of oxidative metabolism, which is exacerbated in retinopathy of prematurity by an inadequate ability to scavenge ROS due to reduced levels of antioxidants (35). Clinical studies have evaluated the use of antioxidants, such as vitamins C and E. However, the results have been inconsistent (35, 42), which is likely to be due, at least in part, to these approaches having suboptimal effects in reducing ROS accumulation.

There is considerable interest in the role of the NADPH oxidase (NOX) family in a wide range of ischemic and ROS-mediated vascular pathologies (3, 5, 17, 59). This is due to the uniqueness of this enzyme family as they are the only enzymes with their sole function being the generation of ROS. Seven isoforms of the NADPH oxidase catalytic unit, NOX (NOX1–5, DUOX1, DUOX2), have been identified, of which NOX1, NOX2, and NOX4 are considered to be relevant to vasculopathy (3, 5, 17, 56, 59). Strategies to reduce NOX activity and the generation of ROS, such as naturally occurring flavonoids, have recently been shown to have benefits in retinal pathology (7, 25). However, the relative contribution of individual NOX isoforms to retinal neovascularization is not known. Identifying the pathologically relevant NOX isoform(s) has the potential to provide a new and effective preventative treatment approach for retinopathy of prematurity. Furthermore, the advent of more specific pharmacological approaches to inhibit certain NOX isoforms, such as GKT137831, represents a new treatment strategy. Indeed, this compound is an orally active NOX inhibitor with a relative specificity for NOX1 and NOX4 (4, 19).

To determine the contribution of NOX isoforms to retinopathy of prematurity, we used a robust *in vivo* model known as oxygen-induced retinopathy (OIR). We induced OIR in mice with deletions of the NOX1, NOX2, or NOX4 isoforms and also evaluated the effects of GKT137831 in mice and rats with OIR. Vascular injury and inflammation as well as the levels of proangiogenic and proinflammatory markers and ROS were examined in retina. To determine the cellular source of NOX in retina, we studied primary cultures of retinal vascular and neuro-glial elements and examined the effects of GKT137831 on hypoxic-induced ROS production in retinal microglia. We have clearly identified NOX1 as the first molecular treatment target for vasculopathy and the excessive production of ROS in retinopathy of prematurity. Our findings therefore have implications for the treatment of various ischemic retinopathies.

Results

Body weight gain

As reported previously, the body weight gain of animals with OIR was reduced compared to room air controls (14). There was no effect of NOX1 and NOX4 isoform deletion on body weight gain. However, NOX2 knockout (KO) mice with OIR had reduced body weight gain compared to NOX2 WT OIR mice. GKT137831 had no effect on body weight gain compared to untreated OIR rats (Supplementary Table S1; Supplementary Data are available online at www.liebertpub.com/ars).

NOX1 KO mice with OIR exhibit reduced retinal neovascularization, vaso-obliteration, and vascular leakage

To determine if NOX1, NOX2, and NOX4 are present in retina, we qualitatively evaluated gene expression in C57BL/6 mice. Given that all the three isoforms were expressed (Fig. 1A), we next determined which NOX isoform contributes to vasculopathy in OIR. Therefore, we studied NOX1 KO, NOX2 KO, and NOX4 KO mice. We first determined that retina from NOX KO mice exhibited a deficiency in the relevant NOX isoform (Fig. 1A) and KO mice did not have compensatory changes in NOX isoform expression (Supplementary Fig. S1A–C). In room air controls, vascularization of the retina was normal. As expected, in all WT mice with OIR, retinal neovascularization and an avascular vaso-obliterated central retina were present (Fig. 1B–D). In NOX1 KO mice with OIR, retinal neovascularization and the avascular central retina were clearly markedly reduced compared to NOX1 WT mice with OIR. However, in NOX2 KO mice and NOX4 KO mice with OIR, neovascularization and the avascular central retina were not reduced compared to respective WT OIR (Fig. 1B–D). The findings for neovascularization were confirmed in paraffin sections of retina (Supplementary Fig. S2A, B). Breakdown of the blood–retinal barrier and subsequent vascular leakage is a major contributor to vision loss (16, 39). Indeed, retinal vascular leakage occurred in WT mice with OIR compared to room air controls (Fig. 1E). In NOX1 KO mice with OIR, retinal vascular leakage was reduced compared to NOX1 WT controls with OIR. However, in NOX2 KO mice and NOX4 KO mice with OIR, retinal vascular leakage was not affected compared to respective WT mice with OIR (Fig. 1E).

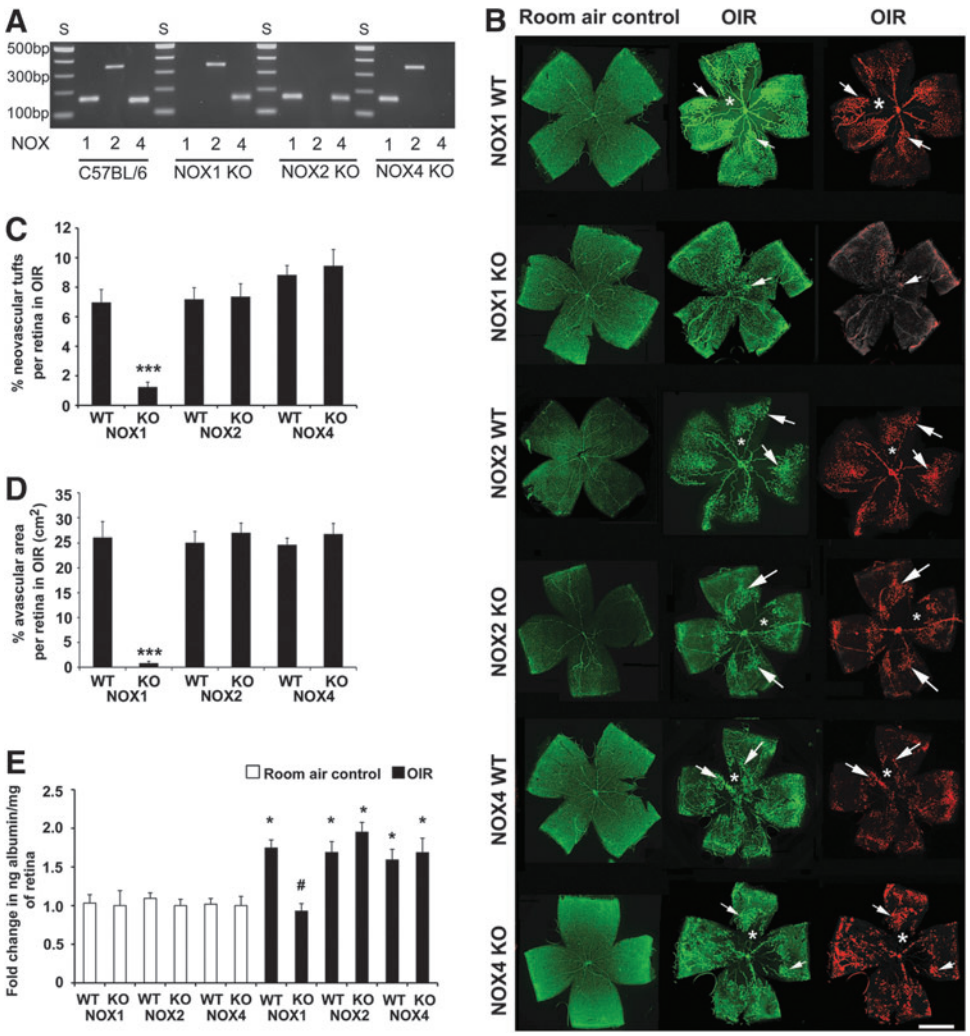

FIG. 1. In OIR, NOX1 KO mice, but not NOX2 KO and NOX4 KO mice, exhibit reduced retinal vasculopathy. (A) NOX1, NOX2, and NOX4 mRNAs were detected in C57BL/6 mouse retina but were absent in retinas from their respective KO strains. S, 100 bp ladder. Mouse NOX1, 168 bp; NOX2, 351 bp; NOX4, 156 bp. **(B)** Retinal wholemounts were labeled with fluorescein isothiocyanate-lectin to show vascularization (green). In OIR groups, the same image is psuedocolorized to show neovascularization (red). In room air control WT and KO mice, neovascularization and an avascular retina were not present. In WT mice with OIR, neovascular tufts (*arrows*) were detected in the mid-periphery, and the central retina (*asterisk*) was avascular. In NOX1 KO mice with OIR, neovascular tufts were reduced by 82% **(C)** and the avascular retina was reduced by 97% **(D)** compared with NOX1 WT mice with OIR. In NOX2 KO and NOX4 KO mice with OIR, neovascular tufts and the avascular retina were not reduced compared to respective WT OIR mice. Original magnification, ×100. Scale bar, 0.25 mm. ***$p < 0.005$ to NOX1 WT OIR. $n = 7$–9 mice per group. Three litters per group were evaluated. **(E)** In WT mice with OIR, retinal vascular leakage was increased compared to room air controls. Only in NOX1 KO mice with OIR was retinal vascular leakage reduced compared to respective WT OIR mice. *$p < 0.05$ to respective room air controls. #$p < 0.05$ to NOX1 WT OIR. $n = 6$–8 mice per group. Values are mean ± SEM. NOX, NADPH oxidase; OIR, oxygen-induced retinopathy; KO, knockout.

NOX1 KO mice with OIR exhibit reduced leukostasis

As inflammation is known to contribute to the development of vasculopathy in OIR (23, 29, 61), we evaluated the extent of leukocyte adherence to the retinal vasculature. In room air controls, few adherent leukocytes were detected in retinal blood vessels (Fig. 2A, B). As expected, in WT mice with OIR, retinal leukostasis was increased compared to room air controls (Fig. 2A, B). Importantly, in NOX1 KO mice with OIR, retinal leukostasis was reduced compared to NOX1 WT mice with OIR to the level seen in room air controls. However, in NOX2 KO and NOX4 KO mice with OIR, retinal leukostasis was not reduced compared to respective WT OIR mice (Fig. 2A, B).

NOX1 KO mice with OIR exhibit reduced labeling for the microglial marker, ionizing binding adaptor molecule-1

Microglia are resident inflammatory cells of the retina, which contribute to vascular remodeling in OIR (43) and are known source of ROS (55). Using the microglial marker, ionizing binding adaptor molecule-1 (Iba1), we investigated the degree of immunolabeling in the region of the retina

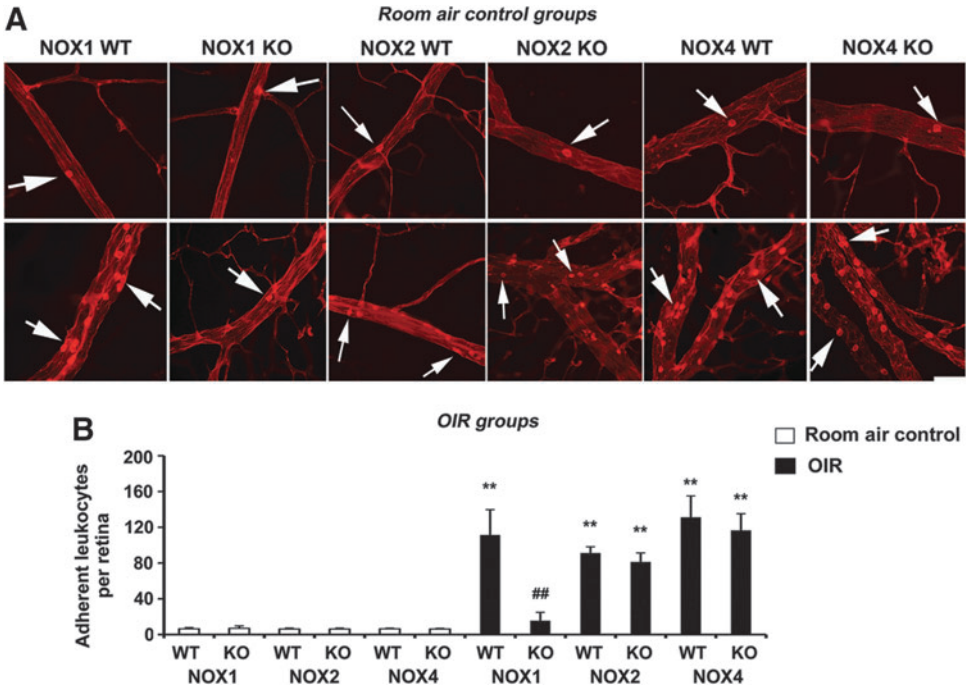

FIG. 2. In OIR, retinal leukostasis is reduced in NOX1 KO mice but not in NOX2 KO and NOX4 KO mice. Leukocytes were identified with rhodamine-concanavalin A. **(A)** In room air control WT mice, few adherent leukocytes (*arrows*) are present. **(A, B)** In WT mice with OIR, leukostasis was increased compared to room air controls. **(A, B)** Only in NOX1 KO mice with OIR was leukostasis reduced compared to respective WT OIR. Original magnification, ×100. Scale bar, 35 μm. Values are mean ± SEM. $^{**}p < 0.01$ to respective room air control groups. $^{\#\#}p < 0.01$ to NOX1 WT OIR. $n = 5$–6 mice per group.

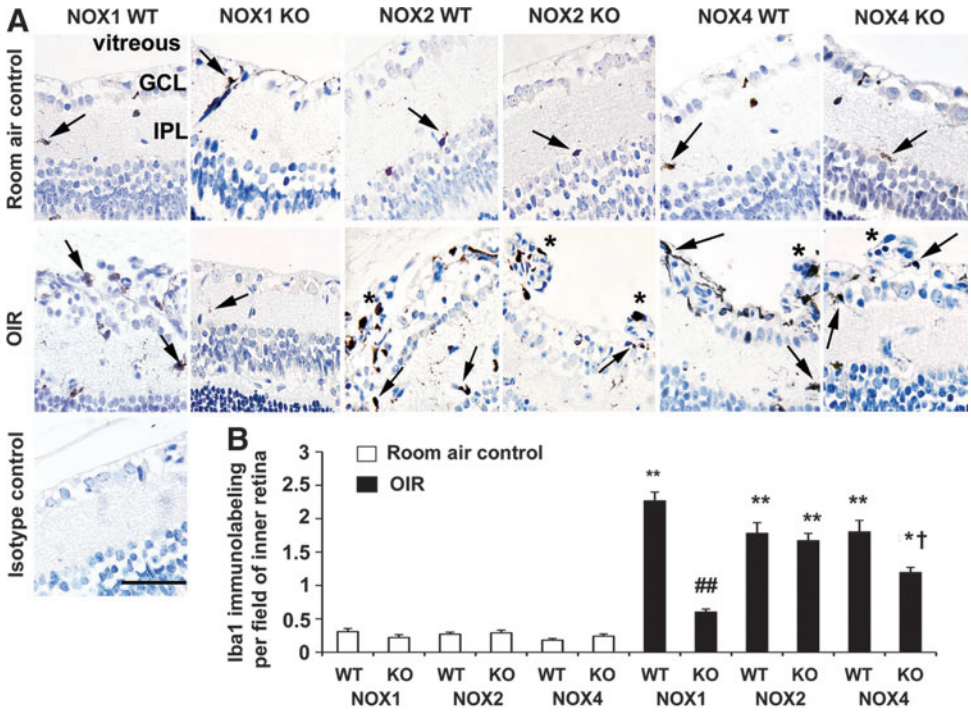

FIG. 3. In OIR, immunolabeling for the microglial marker, Iba1, is markedly reduced in NOX1 KO mice but not in NOX2 KO and NOX4 KO mice. (A) In WT mice with OIR, Iba1 immunolabeling was increased compared to room air controls and often associated with blood vessels (*) at the retinal surface. **(A, B)** In NOX1 KO mice with OIR, Iba1 immunolabeling was markedly reduced compared to NOX1 WT mice with OIR. **(A, B)** In NOX2 KO mice with OIR, Iba1 immunolabeling was similar to NOX2 WT mice with OIR and associated with pre-retinal vessels protruding into the vitreous cavity. In NOX4 KO mice with OIR, Iba1 immunolabeling was slightly reduced compared to NOX4 WT mice with OIR, although still present in pre-retinal blood vessels. Original magnification, ×400. Scale bar, 60 μm. Counterstain, hematoxylin. Values are mean ± SEM. $^{*}p < 0.02$ to respective room air controls. $^{**}p < 0.01$ to respective room air controls. $^{\#\#}p < 0.01$ to NOX1 WT OIR. $^{\dagger}p < 0.02$ to NOX4 WT OIR. $n = 5$–6 mice per group. GCL, ganglion cell layer; IPL, inner plexiform layer; Iba1, ionizing binding adaptor molecule-1.

associated with pre-retinal neovascularization. As previously reported (14), the degree of Iba1 immunolabeling was increased in WT mice with OIR compared to room air controls. Immunolabeling for Iba1 was often associated with blood vessels (Fig. 3A, B). In NOX1 KO mice with OIR, Iba1 immunolabeling did not increase as seen in NOX1 WT mice with OIR (Fig. 3A, B). In NOX2 KO mice with OIR, the extent of Iba1 immunolabeling was similar to NOX2 WT mice with OIR, with this labeling associated with pre-retinal blood vessels. In NOX4 KO mice with OIR (Fig. 3A, B), Iba1 immunolabeling was not elevated to the same extent as NOX4 WT mice with OIR, although still present in pre-retinal blood vessels.

NOX1 KO mice with OIR exhibit reduced expression of angiogenic and inflammatory factors

To determine if angiogenic and inflammatory factors, which are known to be involved in the development of OIR (6, 8, 37, 40), were reduced in the KO mice, we studied the gene expression of VEGF, erythropoietin, angiopoietin-2, and intercellular adhesion molecule-1 (ICAM-1) in retina by quantitative polymerase chain reaction (PCR). As expected, in WT mice with OIR, retinal mRNA levels of all factors were increased compared to room air controls (Fig. 4A–D). Consistent with the decrease in retinal vasculopathy and leukostasis, in NOX1 KO mice with OIR, retinal mRNA levels of these particular molecules implicated in angiogenesis and inflammation, were reduced compared to NOX1 WT mice with OIR (Fig. 4A–D). By contrast, in NOX2 KO and NOX4 KO mice with OIR, the mRNA levels of all these factors were unaltered compared to respective WT mice with OIR (Fig. 4A–D).

NOX1 KO mice with OIR exhibit reduced retinal VEGF protein

Given VEGF's predominant role in retinal vasculopathy and inflammation in OIR (40), we performed VEGF immunolabeling. In room air controls, VEGF immunolabeling was barely detectable and mainly observed on the inner limiting membrane and occasionally in ganglion cells (Fig. 5A). In WT mice with OIR, intense VEGF immunolabeling was observed in pre-retinal neovascular vessels protruding into the vitreous cavity, in some intraretinal blood vessels, ganglion cells, and processes of macroglial Müller cells. In NOX1 KO mice with OIR, but not in NOX2 KO and NOX4 KO mice with OIR, VEGF labeling in all regions was markedly reduced compared to respective WT mice with OIR (Fig. 5A, B).

NOX1 KO mice with OIR exhibit reduced levels of ROS in retina

We next evaluated whether the improvements in OIR that occurred in NOX1 KO mice were accompanied by a reduction in ROS levels in the retina. As expected in all groups, dihydroethidium (DHE) labeling for ROS was present in regions of high oxygen consumption, such as the outer nuclear layer (photoreceptor nuclei) and the inner nuclear layer (mainly macroglial Müller cell nuclei) (Fig. 6A). However, in WT mice with OIR, DHE labeling was also detected in the area of pre-retinal neovascularization at the retinal surface (inner limiting membrane and ganglion cell layer) (Fig. 6A). Consistent with our findings of a reduction in neovascularization in NOX1 KO mice with OIR, retina from these mice exhibited reduced DHE labeling in the region of pre-retinal neovascularization

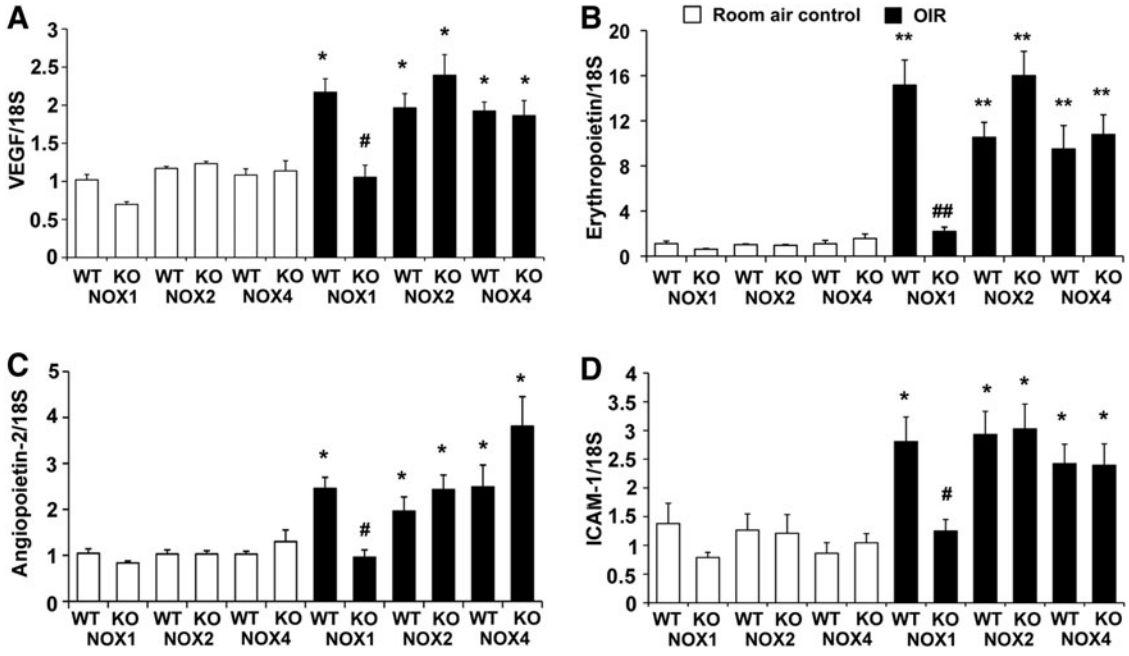

FIG. 4. In OIR, quantitative PCR of retina showed that NOX1 KO mice, but not NOX2 KO and NOX4 KO mice, exhibited reduced mRNA levels of angiogenic and inflammatory factors in retina. In WT mice with OIR, VEGF **(A)**, EPO **(B)**, angiopoietin-2 **(C)**, and ICAM-1 **(D)** mRNA levels in retina were increased compared to room air controls. Only in NOX1 KO mice with OIR were the mRNA levels of these factors reduced compared to respective WT OIR and to the level of room air controls. $^{*}p<0.05$ to respective room air controls. $^{*}p<0.05$ and $^{**}p<0.01$ to respective room air controls. $^{\#}p<0.05$ and $^{\#\#}p<0.01$ to NOX1 WT OIR. $n=6$–10 mice per group. Values are mean ± SEM. ICAM-1, intercellular adhesion molecule-1; VEGF, vascular endothelial growth factor; EPO, erythropoietin; PCR, polymerase chain reaction.

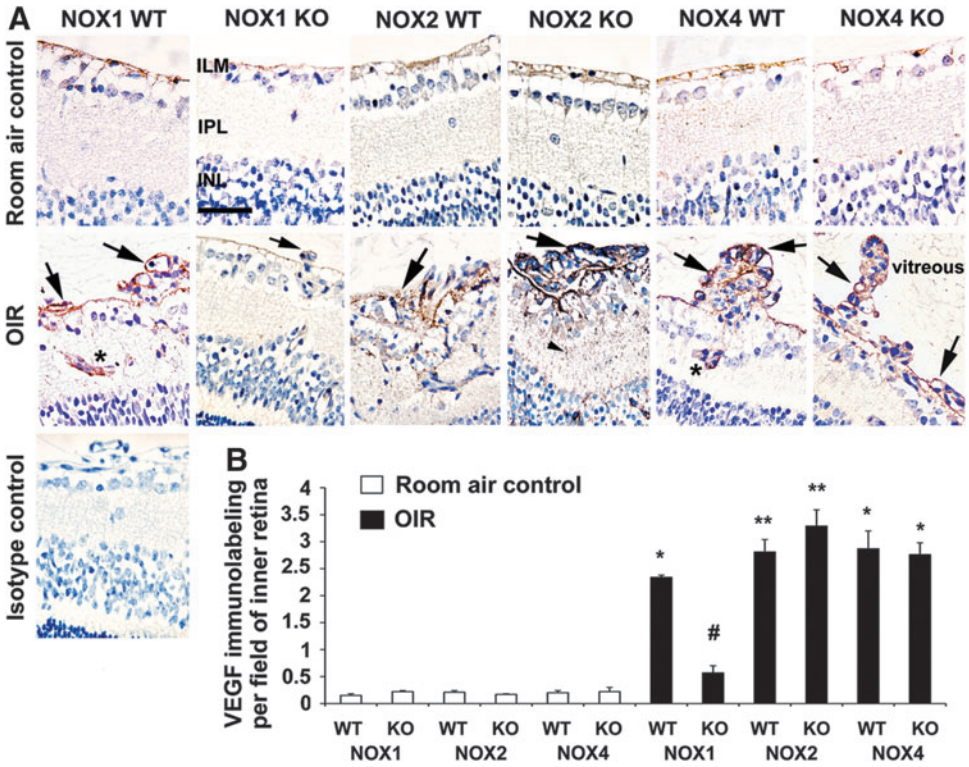

FIG. 5. In OIR, VEGF immunolabeling is reduced in the inner retina of NOX1 KO mice but not in NOX2 KO and NOX4 KO mice. (A) In room air controls, VEGF immunolabeling was present on the retinal surface (ILM). In WT mice with OIR, intense VEGF immunolabeling was present in pre-retinal blood vessels (*arrows*) protruding into the vitreous cavity, some intraretinal blood vessels in the IPL (*asterisk*) and Müller cell processes in the IPL (*arrowhead*) and INL. **(A, B)** Only in NOX1 KO mice with OIR was VEGF immunolabeling reduced compared to WT OIR. In NOX2 KO and NOX4 KO mice with OIR, VEGF immunolabeling was similar to respective WT OIR. Original magnification, ×400. Scale bar, 35 μm. Values are mean ± SEM. *$p < 0.05$ and **$p < 0.01$ to respective room air controls. $^{\#}p < 0.05$ to NOX1 WT OIR. $n = 5$–6 mice per group. ILM, inner limiting membrane; INL, inner nuclear layer.

compared to WT mice with OIR (Fig. 6A, B). However, in NOX2 KO and NOX4 KO mice with OIR and pronounced retinal neovascularization, DHE labeling persisted in the region of neovascularization (Fig. 6A, B). Similar to findings for DHE labeling, we found that labeling for nitrotyrosine, a marker of peroxynitrite-induced damage, was localized to pre-retinal blood vessels in WT mice with OIR and was virtually absent in retina from room air controls (Fig. 7A, B). This pattern of labeling is consistent with previous reports in the OIR model (53). In NOX1 KO mice with OIR, but not in NOX2 KO and NOX4 KO mice with OIR, nitrotyrosine labeling was reduced compared to respective WT mice with OIR (Fig. 7A, B).

GKT137831 inhibited hypoxia-induced ROS generation by microglia and reduced retinal vasculopathy in OIR

As it is not clear which retinal cell populations express particular NOX isoforms, we evaluated NOX expression profiles in primary retinal cultures. A qualitative rather than quantitative assessment was required as retina and cultures were obtained from different species (rats and cows). Studies were not performed in mouse retinal cells as the small size of the neonatal mouse retina hinders the acquisition of a sufficient number of cells for culture. In cultures of retinal rat microglia, ganglion cells and pericytes, NOX1, NOX2, and NOX4, were expressed, whereas cultured retinal glia expressed NOX1 and NOX4 and cultured retinal bovine endothelial cells expressed NOX2 and NOX4 (Fig. 8A–C). Previously, the role of NOX5 has not been evaluated in retina due to its absence from rats and mice, although it is present in other mammals, including humans and cows (59). As NOX5 may be relevant to vascular pathology (21), we evaluated its expression in human retina and in bovine retinal endothelial cells and bovine retinal pericytes. NOX1, 2, 4, and 5 were present in human retina (Supplementary Fig. S3A), and NOX5 was present in both bovine retinal endothelial cells and pericytes (Supplementary Fig. S3B).

Based on our findings that retinal microglia express NOX1, NOX2, and NOX4, and that NOX1 contributes to vasculopathy in OIR, we examined whether microglia are a source of ROS. We exposed primary cultures of microglia to hypoxia to mimic the *in vivo* environment of OIR. Hypoxia for 4 h resulted in increased levels of ROS in cell lysates compared to normoxia controls. GKT137831 reduced the elevated ROS levels to that of normoxia controls (Fig. 8D). We next determined if GKT137831 reduced vasculopathy in OIR. In OIR rats, and NOX4 WT and KO mice, GKT137831 reduced neovascularization and the avascular retina compared to untreated OIR animals (Fig. 8E–J). Both early intervention and late intervention were equally effective in rats with OIR (Fig.

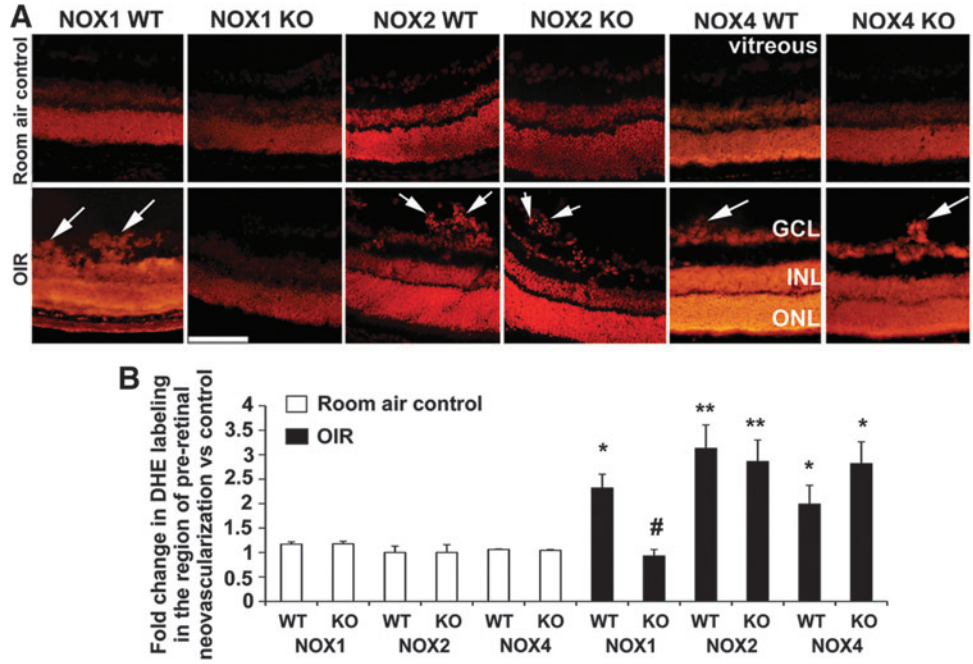

FIG. 6. In OIR, NOX1 KO mice, but not NOX2 KO and NOX4 KO mice, have reduced ROS in the region of pre-retinal neovascularization. (A) In all groups, DHE labeling for ROS was present in the outer retina in the ONL and INL. However, in WT mice with OIR, DHE labeling was also present at the retinal surface on pre-retinal blood vessels protruding into the vitreous cavity (*arrows*) and in the GCL. **(A, B)** In NOX1 KO mice with OIR, DHE labeling was barely detectable at the retinal surface and GCL. In NOX2 KO and NOX4 KO mice with OIR, DHE labeling was present on pre-retinal blood vessels. Original magnification, ×200. Scale bar, 70 μm. Values are mean ± SEM. *$p < 0.05$ and **$p < 0.01$ to respective room air controls. #$p < 0.05$ to NOX1 WT OIR. $n = 5$–6 mice per group. ONL, outer nuclear layer; DHE, dihydroethidium; ROS, reactive oxygen species.

8H–J). GKT137831 also reduced the levels of DHE labeling in C57BL/6 mice with OIR (Supplementary Fig. S4).

Discussion

The present study provides the first evidence that NOX1, but not NOX2 or NOX4, has an important role in the development of OIR. Using mice with genetic deficiencies in NOX isoforms, we demonstrated that deletion of NOX1, but not NOX2 or NOX4, protected against OIR-induced retinal neovascularization, capillary vaso-obliteration, vascular leakage, and vascular adherence of leukocytes. Furthermore, NOX1 KO mice exhibited in retina reduced the expression of proangiogenic and proinflammatory factors as well as reduced microglial density and ROS levels. The novel dual NOX1 and NOX4 inhibitor, GKT137831, reduced retinal vasculopathy in mice and rats with OIR and also in NOX4 KO mice with OIR. We determined that the vascular and neuroglial elements involved in the development of retinal vascular injury in retinopathy of prematurity are sources of NOX1, 2, and 4 and that NOX5 is present in human retina. Furthermore, we identified microglia as a source of hypoxia-induced ROS generation, which is responsive to GKT137831. This is the first report to provide direct evidence that NOX1 has a pathological role in OIR, a finding that has major implications for the medical treatment of retinopathy of prematurity and other neovascular ischemic retinopathies.

Vision loss and blindness caused by retinopathy of prematurity is largely a consequence of hypoxia-induced neovascularization and vascular leakage (10). VEGF is arguably the most important mediator of this pathology (30), with contributions from other factors, such as erythropoietin (9) and angiopoietin-2 (37). Our data revealed a predominant role for NOX1 in promoting the expression of these putative mediators of OIR. Few studies have compared the role of NOX isoforms in angiogenesis *in vivo* (17, 56), and to our knowledge, none have been performed in retinopathy. Our findings are in agreement with other studies investigating the role of NOX isoforms in angiogenesis, although these experiments were performed in other organs. For example, basic fibroblast growth factor-stimulated angiogenesis in matrigel plugs was reduced in NOX1 KO mice but not in NOX2 KO or NOX4 KO mice (17). A key role for NOX1 in angiogenesis has also been reported in tumors where NOX1 was suggested to be the angiogenic switch for VEGF-related vascular growth (5). These results for NOX1 contrast those studies that showed angiogenic functions for NOX2 and NOX4. In NOX2 KO mice with VEGF-loaded sponge implants, angiogenesis was reduced (54). Angiogenesis was blunted in NOX4 KO mice with femoral artery ligation (47), whereas in cardiomyocyte-specific NOX4 overexpressing mice, myocardial capillary density was increased (62). The reasons for the divergent angiogenic roles of the NOX isoforms are not clear; however, it is possible that the influence of particular NOX isoforms on angiogenesis depends on the tissue environment. In this regard, it can be speculated that the drivers for neovascularization in OIR, namely intense hypoxia and contributions from inflammatory cells (23, 43), favor NOX1 over other NOX

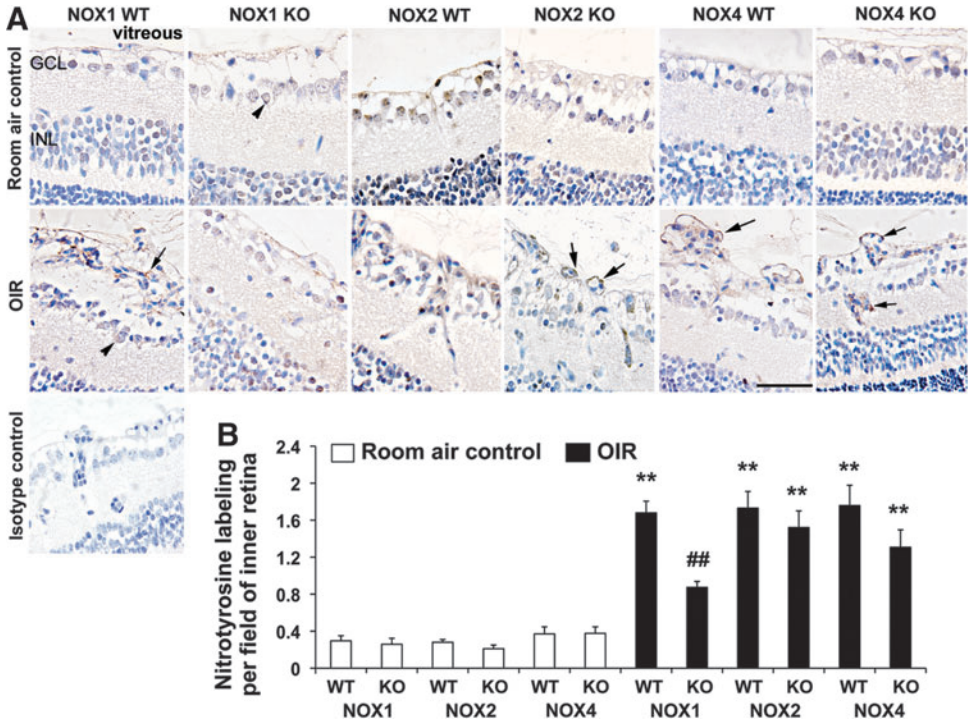

FIG. 7. In OIR, NOX1 KO mice, but not NOX2 KO and NOX4 KO mice, exhibit reduced nitrotyrosine levels in the inner retina. Three-micrometer paraffin sections of retinas were counterstained with hematoxylin. **(A)** In WT mice, immunolabeling for nitrotyrosine is barely detected and occasionally observed in ganglion cells (*arrowheads*) in the GCL and in the INL. In WT OIR mice, intense immunolabeling for nitrotyrosine is observed in these regions and also in pre-retinal blood vessels (*arrows*) that protrude into the vitreous cavity. In NOX1 KO mice with OIR, pre-retinal blood vessels are absent and therefore nitrotyrosine labeling is not apparent, whereas in NOX2 and NOX4 KO mice with OIR, immunolabeling is found on pre-retinal blood vessels. Original magnification, $\times 400$. Scale bar, 60 μm. **(B)** Values are mean $\pm$ SEM. $^{**}p < 0.01$ to respective room air controls. $^{\#\#}p < 0.01$ to NOX1 WT OIR. $n = 5$ mice per group.

isoforms. Of interest are the mechanisms by which hypoxia influences NOX1 expression and activity. Furthermore, it will be important to determine how NOX1 expression and activity influence the production of angiogenic and inflammatory genes during the development of OIR, and particularly the contribution of hypoxic-inducible factor-1α, which is upregulated in the acute stage of OIR (34).

The early stage of OIR in mice features hyperoxia-induced capillary vaso-obliteration resulting in an avascular central retina. The extent of damage is viewed to predict the severity of neovascularization in OIR (28). Elevated levels of ROS are thought to be involved in this capillary degeneration as intravitreal administration of liposome-encapsulated superoxide dismutase (36) and systemically administered Trolox, a water-soluble analogue of vitamin E (39), reduce the avascular area in OIR. Our data extend these findings by highlighting that NOX1, but not NOX2 or NOX4, is likely to be a source of ROS, which mediates capillary degeneration in OIR.

Leukocytes contribute to OIR by remodeling the retinal vasculature and/or delivering inflammatory mediators, cytokines and possibly ROS to influence neovascularization (23, 43). In OIR, leukocytes adhere to the retinal vasculature (58). We demonstrated that a deficiency in NOX1, but not in NOX2 or NOX4, reduces retinal leukostasis in OIR. Furthermore, there was a reduction in ICAM-1 levels in NOX1 KO mouse retina consistent with the previously reported major role of ICAM-1 in retinal leukostasis (32). To our knowledge, little is known about the contribution of NOX2 and NOX4 to retinal inflammation in OIR. It has been reported that lipopolysaccharide-induced as well as diabetes-induced leukostasis and ICAM-1 expression were reduced in NOX2 KO mice (2). The reasons for the differences between these findings and our results may, as previously mentioned, relate to the particular retinal disease being evaluated. However, it is possible that given NOX2's role in inflammation (41, 48), it may influence inflammatory processes in the early stages of OIR. Nevertheless, strategies to inhibit NOX2 in patients are not likely to be appropriate since deficiencies in NOX2 are associated with compromised phagocytic defense resulting in life-threatening bacterial and fungal infections (48), a situation that could have severe consequences for children with retinopathy of prematurity who are already prone to infections (29).

Several reports have shown that ROS levels are increased in the retina after OIR (1, 6, 44, 53) and that untargeted scavenging of ROS with agents such as vitamin C derivatives and the nonspecific NOX inhibitor, apocynin (49), reduce retinal neovascularization and vaso-obliteration (1, 44). Consistent with previous studies (1, 53), we found increased ROS levels in WT mice with OIR in the region of pre-retinal neovascularization. Importantly, we also demonstrated that a deficiency in NOX1, but not in NOX2 and NOX4, reduced this increase in ROS levels. This finding was substantiated in WT mice with OIR, where ROS levels in the inner retina were reduced with GKT137831. A previous study in OIR reported

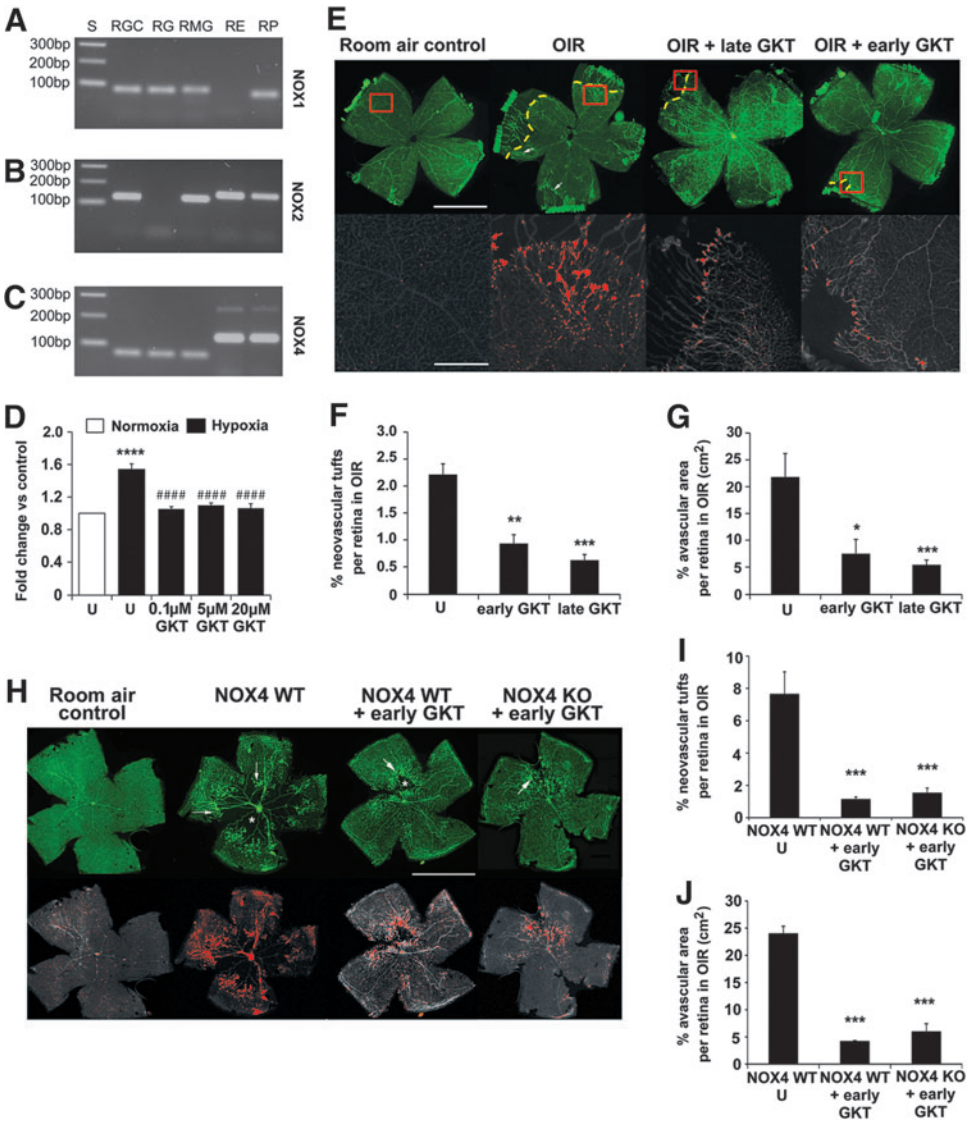

FIG. 8. GKT137831 (GKT) inhibited hypoxia-induced ROS generation by microglia and reduced retinal vasculopathy in OIR. NOX1 **(A)**, NOX2 **(B)**, and NOX4 **(C)** expression was detected in rat RMG, rat RGC, and bovine RP. NOX1 and NOX4, but not NOX2, were present in rat RG. NOX2 and NOX4, but not NOX1, were present in bovine RE. S, 100 bp ladder. Rat NOX1, 82 bp; bovine NOX1, 67 bp; rat NOX2, 131 bp; bovine NOX2, 152 bp; rat NOX4, 71 bp; bovine NOX4, 130 bp. **(D)** In microglial cell lysates, hypoxia increased ROS levels (DHE) compared to normoxia control. In microglial exposed to hypoxia, GKT reduced ROS to the level of normoxia control. $^{****}p < 0.0001$ to normoxia-untreated (U) control. $^{\#\#\#\#}p < 0.0001$ to hypoxia-untreated control. $n = 3$–4 independent experiments with triplicate samples within each experiment. **(E)** Retinal wholemounts from Sprague Dawley rats were labeled with fluorescein isothiocyanate (FITC)-lectin to show vascularization (green). Original magnification, ×100. Scale bar, 0.4 mm. Regions from each image are enlarged (boxes) and psuedocolorized to show neovascularization (red). Original magnification, ×100. Scale bar, 0.04 mm. In room air controls, neovascularization and an avascular retina were not present. In untreated (U) OIR, neovascular tufts (*arrows*) were detected in the mid-periphery, and regions of the peripheral retina (marked by the *yellow dotted line*) were avascular. In rats with OIR, both early and late treatment with GKT reduced neovascular tufts **(F)** and the avascular retina **(G)** compared to untreated OIR. $^{*}p < 0.02$ to untreated OIR. $^{**}p < 0.01$ to untreated OIR. $^{***}p < 0.005$ to untreated OIR. $n = 6$–7 rats per group. **(H)** Retinal wholemounts from NOX4 WT and KO mice were labeled with FITC-lectin to show vascularization (green). Images were psuedocolorized to show neovascularization (red). Original magnification, ×100. Scale bar, 0.4 mm. In NOX4 WT room air controls, neovascularization and an avascular retina were not present. In NOX4 WT OIR mice that were untreated (U), neovascular tufts (*arrows*) were detected in the mid-periphery, and the central retina was avascular (*asterisk*). In NOX4 WT and KO mice with OIR, early treatment with GKT reduced neovascular tufts **(I)** and the avascular retina **(J)** compared to untreated OIR. $^{***}p < 0.001$ to untreated OIR. $n = 8$–11 mice per group. Values are mean ± SEM. RMG, retinal microglial; RGC, retinal ganglion cells; RP, retinal pericytes; RG, retinal glia; RE, retinal endothelial cells.

that ROS levels were reduced when retinal sections were incubated with NOX2-tat (a peptide that inhibits NOX assembly by binding to p47phox and blocking its interaction with NOX2) (1). However, despite these reported results, we did not find a reduction in retinal vasculopathy in NOX2 KO mice with OIR, suggesting that any ROS generated from NOX2 is likely to have little impact on retinal neovascularization. Indeed, it remains controversial as to whether NOX2-tat is specific for NOX2 (59), and thus, its effects may also be mediated by inhibition of NOX1.

To determine whether the inhibition of NOX isoforms is a potential treatment of retinopathy of prematurity, we chose a complementary pharmacological approach by evaluating the NOX inhibitor, GKT137831, which inhibits both NOX1 and NOX4. Studies were performed in NOX4 KO mice with OIR and also in rats with OIR as the retinopathy, which develops in rats, more closely mimics that of children with retinopathy of prematurity (22). GKT137831 had a similar effect to NOX1 deletion in suppressing retinal neovascularization and reducing the extent of loss of retinal avascularity in OIR. These findings demonstrate the potential of specific NOX isoform inhibition as a treatment of retinopathy of prematurity in children.

Neovascularization in OIR is largely driven by the hypoxia-induced upregulation of VEGF and other angiogenic factors produced in neurons and glia (52). Therefore, the next logical step would be to determine the cellular location of NOX isoforms in retina. However, this is difficult due to the paucity of reliable and specific NOX antibodies. Furthermore, antibody approaches are unlikely to provide information about the activities of individual NOX isoforms. We therefore performed a qualitative assessment of NOX isoform mRNA levels in primary cultures of retinal cells involved in neovascularization. Under basal conditions, only microglia, ganglion cells, and pericytes expressed NOX1, NOX2, and NOX4. Given that microglia contribute to OIR (43) and are important producer of ROS and cytokines (50, 55), further evaluation of this particular cell type was performed. In OIR, immunolabeling for retinal microglia in the inner retina was reduced in NOX1 KO mice but remained elevated in NOX2 KO and NOX4 KO mice, although there was a small reduction in NOX4 KO mice. However, the presence of microglia in the neovascular tufts of retina from NOX4 KO mice with OIR may indicate why retinal neovascularization was not reduced in these animals. We complemented these *in vivo* studies by demonstrating that hypoxia induces the increased production of ROS in cultured microglia. The ability of GKT137831 to suppress this increase in ROS confirms the role of NOX in excess ROS formation in microglia. However, these findings do not preclude a role for retinal cells other than microglia as a source of ROS derived from NOXs that contribute to retinal neovascularization in OIR. For instance, a recent study has shown that retinal ganglion cells exhibit a preferential increase in NOX1 mRNA rather than NOX2 and NOX4 mRNA after ischemia (15).

In summary, retinopathy of prematurity is the major ocular condition causing blindness of the neonate, and its prevalence has escalated due to the increased survival of younger and smaller babies. Currently, there are no effective strategies that prevent or attenuate the vasculopathy of this vision-threatening disorder. Although anti-VEGF therapies have been suggested as a treatment option, there are concerns about detrimental effects of such a treatment approach on retinal and organ development (13). Our data provide the first evidence that NOX1 influences retinal vasculopathy in OIR by the increased production of ROS and subsequent generation of angiogenic and inflammatory factors (Fig. 9). NOX1 inhibition has the potential to become an effective

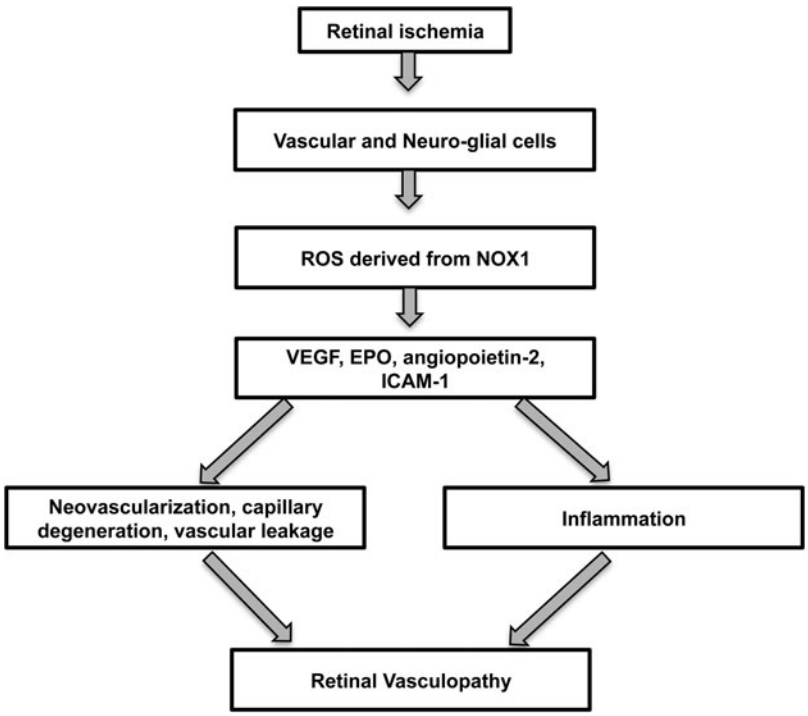

FIG. 9. Schematic diagram showing the possible involvement of NOX1 in vascular pathology in the retina. Ischemic retinopathies may lead to the increased generation of ROS derived from NOX1 from vascular and neuro-glial cells. This results in the production of angiogenic and inflammatory factors, such as VEGF, EPO, angiopoietin-2, and ICAM-1. These factors promote neovascularization, capillary degeneration, and vascular leakage as well as inflammation to result in retinal vasculopathy and compromised vision.

mechanism-based treatment strategy by alleviating the increases in pathologically relevant ROS. Certainly, further studies evaluating the effects of NOX1 inhibition and GKT137831 on other aspects of retinal pathology including neuronal and glial dysfunction are necessary before these findings can be translated to patients. Furthermore, the ocular safety profiles of NOX isoform inhibitors such as GKT137831 in patients with retinopathy will need to be established. Finally, a role for NOX5 in ischemic retinopathy cannot be entirely excluded given that it is expressed in human retina and bovine retinal vascular cells, but unfortunately at present cannot be studied in relevant rodent models. Overall, our findings are not only relevant for retinopathy of prematurity but also for other retinopathies and organ pathologies that feature neovascularization associated with amplified ROS.

Materials and Methods

Animals

All procedures were approved by the Alfred Medical Research and Education Precinct (AMREP) animal ethics committee and performed according to the National Health and Medical Research Council (NHMRC) of Australia's Guidelines for the Care of Animals in Scientific Research. In rodents, OIR develops over two phases comprising vaso-obliteration (Phase I) and neovascularization (Phase II) (40). In mice, Phase I was induced using a previously published protocol with a minor modification (57). Mice were exposed between postnatal day (P)7 and P11 to 75% O_2 cycled with 20% O_2 for 3 h/day. In rats, Phase I was induced by exposure between P0 and P11 to 80% O_2 cycled with 20% O_2 for 3 h/day (14, 33, 58). Phase II of OIR occurred when mice and rats were placed in room air from P12 to P18. Controls were in room air for the entire study (P0–P18). NOX1 KO, NOX2 KO (Jackson Laboratories, Bar Harbour, ME), and NOX4 KO (26) mice were bred on a C57BL/6 background. WT for NOX1 KO and NOX4 KO were littermates and for NOX2 KO were C57BL/6 mice. NOX1 KO mice were a gift from Professor Karl-Heinze Krause, Geneva, Switzerland (18). Sprague Dawley rats were purchased from the Australia Research Centre (Perth, Western Australia). Rats were treated with GKT137831 at a dose of 60 mg/kg/day between P0 to P18 (early intervention) and P12 to P18 (late intervention). GKT137831 was dissolved in dimethyl sulfoxide and administered by subcutaneous injection (100 μl). Controls received dimethyl sulfoxide by subcutaneous injection (100 μl). A separate set of NOX4 WT and NOX4 KO mice with OIR mice were treated with GKT137831 (60 mg/kg/day) from P7 to P18 by subcutaneous injection (100 μl). GKT137831 was provided by Genkyotex SA (Geneva, Switzerland). Mice and rats were killed at P18 with sodium pentobarbitone (170 mg/ml; Virbac, Peakhurst, New South Wales, Australia).

NOX inhibition

GKT137831, a member of the pyrazolopyridine dione family is an efficient inhibitor of both NOX1 and NOX4 isoforms (Ki in the range of 100–150 n*M* in cell-free assays of ROS production using membranes prepared from cells heterologously overexpressing specific NOX enzyme isoforms) (4). GKT137831 is also a weak inhibitor of the NOX2 isoform in cell-free assays but does not significantly inhibit neutrophil oxidative burst at concentrations up to 100 μM and does not inhibit innate microbial bacterial killing *in vitro* or *in vivo* (when used at a concentration of up to 20 μM or administered at 100 mg/kg orally, respectively). Furthermore, GKT137831 has no scavenging or antioxidant activity when tested at 10 μM and has an excellent specificity for NOX1 and NOX4 enzymes as shown in an extensive *in vitro* off-target pharmacological profiling on 170 different proteins, including ROS producing and redox-sensitive enzymes (24, 27).

Retinal neovascularization and vaso-obliteration in retinal wholemounts

Retinal wholemounts were prepared as described previously (14, 57). More information can be found in Supplementary Data. Seven to nine mice per group were evaluated from three litters of animals, and six to seven rats per group were examined. Neovascularization (neovascular tufts) was defined as clumps of blood vessels that were positively labeled for BS-I lectin. Neovascular tufts over the whole retina were psuedocolorized in red, and Image J software (v3.1; National Institutes of Health, Bethesda, WA) was used to set a threshold for red fluorescent labeling, which was then applied to all sections. Neovascular tufts were quantitated over the whole retina and expressed as a % of neovascular tufts per retina. The extent of vaso-obliteration (avascular area) in the central retina (for mice) and mid-peripheral retina (for rats) was quantitated using the freehand line tool in Image J. The avascular area was expressed as a percentage of the total retinal area. Retinal neovascularization was confirmed in 3-μm paraffin sections from a separate set of NOX1, NOX2, and NOX4 WT and KO mice, as previously described (14, 57).

Retinal vascular leakage and leukostasis

Elevated levels of albumin in retina are an indicator of vascular leakage and blood–retinal barrier breakdown (38). Albumin levels in freshly frozen single retina were measured according to the manufacturer's instructions using a commercially available Mouse Albumin Enzyme-linked immuno sorbent assay quantification set (Bethyl Laboratories, Montgomery, TX). Albumin values were normalized to dry retinal weight. Six to eight mice per group were evaluated. To measure the extent of adherence of leukocytes to the retinal vasculature, leukostasis was quantitated as described previously (57). More information is found in Supplementary Data.

Immunohistochemistry for microglia and VEGF

Immunohistochemistry for the microglial marker, Iba1, and for VEGF was performed as described previously (14). Four 3-μm paraffin sections at least 60 μm apart were randomly selected from each eye, dewaxed in histolene, and hydrated in graded ethanols. Antigen retrieval was achieved by microwaving in 0.1 *M* citrate buffer for 10 min. After washing with 0.1 *M* phosphate-buffered saline (PBS), pH 7.4, sections were incubated with 1% normal goat serum in PBS for 1 h for Iba1 labeling or 10% donkey serum in PBS for 1 h for VEGF labeling. The sections were then incubated overnight at 4°C with either an anti-Iba1 antibody (1:1000; Wako, Tokyo, Japan) or a goat anti mouse VEGF164 antibody (R&D systems, Minneapolis, MN). The sections were washed three times with PBS and incubated for 30 min with either a

biotin-conjugated goat anti-rabbit IgG (1:200; DakoCytomation, Glostrup, Denmark) for Iba1 labeling or a biotinylated donkey anti-goat IgG antibody (1:500; Jackson Immunoresearch, West Grove, PA) for VEGF labeling. After washing with PBS, the sections were then incubated with the Vectastain ABC standard kit (Vector Laboratories, Burlingame, CA) for 30–45 min and liquid DAB + substrate chromagen system (Dakocytomation) for 15 s. The sections were then counterstained with Harris' Haematoxylin for 7 min, rinsed in tap water, dehydrated through graded ethanols, cleared in histolene, and coverslipped with DPX (VWR International Ltd., Poole, England). A negative control without the primary antibody and an isotype IgG antibody control were included to detect nonspecific labeling. In each section, four nonoverlapping fields at ×400 magnification were captured using a Spot digital camera (SciTech, Preston, Victoria, Australia). Image J software was used to set a threshold for brown Iba1 immunolabeling and brown VEGF immunolabeling, which was then applied to all captured fields. Immunolabeling was quantitated using the threshold tool in the inner retina, which included pre-retinal blood vessels attached to the retinal surface and protruding into the vitreous cavity. The inner retina comprised the inner limiting membrane, ganglion cell layer, and inner plexiform layer. Results are expressed as Iba1 or VEGF immunolabeling per field of inner retina. Five to six mice per group were evaluated.

Real-time PCR and qualitative assessment of NOX isoform expression

In mice, this was performed for NOX1, NOX2, NOX4, VEGF, erythropoietin, angiopoietin-2, and ICAM-1, as described previously (14, 57). More information is found in Supplementary Data. Total RNA was isolated from single retinas of 6–10 mice per group. To qualitatively determine the expression profile of the NOX1, NOX2, NOX4, and NOX5 isoforms in distinct retinal cell types, RNA was isolated from cultured rat ganglion cells, glia, and microglia, and bovine retinal endothelial cells and pericytes. The method for the primary culture of rat ganglion cells, glia and bovine retinal endothelial cells and pericytes is described previously (14, 58). NOX isoform expression was qualitatively assessed in a human retinal cDNA preparation (BioChain, Newark, CA). Confirmation of the absence of NOX1 mRNA in NOX1 KO retinas, NOX2 mRNA in NOX2 KO retinas, and NOX4 mRNA in NOX4 KO retinas was achieved from amplifications using primers located within the exonic regions disrupted in each NOX KO mouse strain. The primer sequences used in the study are found in Supplementary Table S2.

Reactive oxygen species

The DHE method was used to measure ROS levels in single retina. Eyes were enucleated and immediately frozen in OCT compound (Sakura Finetechnical Co., Ltd., Tokyo, Japan). Unfixed cryosections (20 μm) were incubated with sterile PBS containing 0.1% D-glucose (Ajax Chemicals, Sydney, Australia), L-arginine (50 μM; Sigma, St. Louis, MO), NADPH (100 μM; Roche Applied Science, IN), and DHE (2 μM; Sigma) for 30 min at 37°C, as previously described (11, 46). These sections were then photographed using an inverted fluorescence microscope (Eclipse TE2000; Nikon Instrument, Inc., Melville, NY) equipped with a digital camera and interfaced with a computer running NIS-Elements version 2.20 (Nikon Instruments, Inc.) in the same exposure conditions; the intensity of the staining was measured using the Image J program (version 1.37; National Institutes of Health). Five mice per group were evaluated. From each animal, three sections were randomly selected and labeling intensity was measured in the region of the retinal surface associated with pre-retinal neovascularization (inner limiting membrane and ganglion cell layer). Immunolabeling for nitrotyrosine was performed as described above (53). Sections were incubated with 0.5% skim milk for 10 min, which was followed by incubation with an anti-nitrotyrosine antibody overnight at 4°C (1:400; Millipore, Temecula, CA). Five animals per group were evaluated.

Primary cultures of rat retinal microglia under hypoxic conditions

The methods for culturing primary rat retinal microglia are as described previously (14). Characterization of cultured retinal microglia was performed with immunohistochemistry for Iba1 (14). Dishes containing purified retinal microglia were placed in a Modular Incubator Chamber (MIC101; QNA International Pty Ltd, Glenferrie South, Victoria, Australia). The hypoxic conditions were established by flushing the chamber for 4 min with 0.5% O_2, 94.5% N_2, and 5% CO_2. The same gas mixture was then pumped into the chamber and immediately the chamber was sealed. Microglia were exposed to GKT137831 at concentrations of 0.1, 5, and 10 μM. The chamber was then placed in a 37°C incubator for 4 h. Comparisons were made to microglia exposed to normoxic conditions.

ROS levels in rat retinal microglial lysates

Primary cultured rat retinal microglia were washed with Hank's balanced salt solution (HBSS) for 2 min followed by a 30-min incubation with 5 μM DHE at 37°C in 5% CO_2, in the dark. After incubation, cells were washed with HBSS and then imaged immediately using an Eclipse TE2000 inverted fluorescence microscope (Nikon Instruments, Inc.) and image-processing computer software (NIS-Elements version 2.20; Nikon Instruments, Inc.). Fluorescence intensity of cells was used as a measure of intracellular ROS levels using Image J analytical software (version 1.44). For quantitation, a minimum of 15 randomly selected cells from three different fields from each dish was evaluated. The intensity of fluorescence in a blank space between two cells was measured as background intensity. Three independent experiments were performed in each group with a minimum of three replicates.

Statistics

All data were analyzed using the GraphPad Prism software (v.5; GraphPad Software, Inc., LA Jolla, CA). Both animal and cell culture data sets were assessed for normality, and in the case of more than two treatments, a one-way ANOVA (parametric) was followed by a Bonferroni *post hoc* analysis or Kruskal–Wallis or by Mann–Whitney *U* tests (nonparametric). Either an unpaired *t*-test (parametric) or a Mann–Whitney *U* test (nonparametric) was conducted when there were only two treatments. Investigators were masked to the groups. A value of $p < 0.05$ was considered significant.

Acknowledgments

The authors thank Mariam Sofi and David R. Berka for technical assistance. The authors thank Monash Micro Imaging for assistance with confocal microscopy. JDRF and the NHMRC of Australia generously supported this research. Both J.L.W.-B. and K.A.J.-D. are NHMRC Senior Research Fellows. M.E.C. is an Australian Fellow of the NHMRC and JDRF Scholar. H.H.H.W.-S. is supported by the EU (Marie Curie International Reintegration Grant and ERC Advanced Grant) and Dutch Kidney Foundation. D.D. was awarded a Postgraduate Publication Award from the Monash University.

Author Disclosure Statement

C.S. is an employee of Genkyotex, Geneva, Switzerland. The other authors have nothing to disclose.

References

1. Al-Shabrawey M, Bartoli M, El-Remessy AB, Platt DH, Matragoon S, Behzadian MA, Caldwell RW, and Caldwell RB. Inhibition of NAD(P)H oxidase activity blocks vascular endothelial growth factor overexpression and neovascularization during ischemic retinopathy. *Am J Pathol* 167: 599–607, 2005.
2. Al-Shabrawey M, Rojas M, Sanders T, Behzadian A, El-Remessy A, Bartoli M, Parpia AK, Liou G, and Caldwell RB. Role of NADPH oxidase in retinal vascular inflammation. *Invest Ophthalmol Vis Sci* 49: 3239–3244, 2008.
3. Altenhofer S, Kleikers PW, Radermacher KA, Scheurer P, Rob Hermans JJ, Schiffers P, Ho H, Wingler K, and Schmidt HH. The NOX toolbox: validating the role of NADPH oxidases in physiology and disease. *Cell Mol Life Sci* 69: 2327–2343, 2012.
4. Aoyama T, Paik YH, Watanabe S, Laleu B, Gaggini F, Fioraso-Cartier L, Molango S, Heitz F, Merlot C, Szyndralewiez C, Page P, and Brenner DA. Nicotinamide adenine dinucleotide phosphate oxidase in experimental liver fibrosis: GKT137831 as a novel potential therapeutic agent. *Hepatology* 56: 2316–2327, 2012.
5. Arbiser JL, Petros J, Klafter R, Govindajaran B, McLaughlin ER, Brown LF, Cohen C, Moses M, Kilroy S, Arnold RS, and Lambeth JD. Reactive oxygen generated by Nox1 triggers the angiogenic switch. *Proc Natl Acad Sci USA* 99: 715–720, 2002.
6. Bartoli M, Al-Shabrawey M, Labazi M, Behzadian MA, Istanboli M, El-Remessy AB, Caldwell RW, Marcus DM, and Caldwell RB. HMG-CoA reductase inhibitors (statin) prevents retinal neovascularization in a model of oxygen-induced retinopathy. *Invest Ophthalmol Vis Sci* 50: 4934–4940, 2009.
7. Bucolo C, Leggio GM, Drago F, and Salomone S. Eriodictyol prevents early retinal and plasma abnormalities in streptozotocin-induced diabetic rats. *Biochem Pharmacol* 84: 88–92, 2012.
8. Chen J, Connor KM, Aderman CM, and Smith LE. Erythropoietin deficiency decreases vascular stability in mice. *J Clin Invest* 118: 526–533, 2008.
9. Chen J, Connor KM, Aderman CM, Willett KL, Aspegren OP, and Smith LE. Suppression of retinal neovascularization by erythropoietin siRNA in a mouse model of proliferative retinopathy. *Invest Ophthalmol Vis Sci* 50: 1329–1335, 2009.
10. Chen J, Stahl A, Hellstrom A, and Smith LE. Current update on retinopathy of prematurity: screening and treatment. *Curr Opin Pediatr* 23: 173–178, 2010.
11. Chen P, Guo AM, Edwards PA, Trick G, and Scicli AG. Role of NADPH oxidase and ANG II in diabetes-induced retinal leukostasis. *Am J Physiol Regul Integr Comp Physiol* 293: R1619–R1629, 2007.
12. Connor KM, SanGiovanni JP, Lofqvist C, Aderman CM, Chen J, Higuchi A, Hong S, Pravda EA, Majchrzak S, Carper D, Hellstrom A, Kang JX, Chew EY, Salem N Jr., Serhan CN, and Smith LE. Increased dietary intake of omega-3-polyunsaturated fatty acids reduces pathological retinal angiogenesis. *Nat Med* 13: 868–873, 2007.
13. Darlow BA, Gilbert C, Quinn GE, Azad R, Ells AL, Fielder A, and Zin A. Promise and potential pitfalls of anti-VEGF drugs in retinopathy of prematurity. *Br J Ophthalmol* 93: 986, 2009.
14. Deliyanti D, Miller AG, Tan G, Binger KJ, Samson AL, and Wilkinson-Berka JL. Neovascularization is attenuated with aldosterone synthase inhibition in rats with retinopathy. *Hypertension* 59: 607–613, 2012.
15. Dvoriantchikova G, Grant J, Santos AR, Hernandez E, and Ivanov D. Neuronal NAD(P)H oxidases contribute to ROS production and mediate RGC death after ischemia. *Invest Ophthalmol Vis Sci* 53: 2823–2830, 2012.
16. Gariano RF and Gardner TW. Retinal angiogenesis in development and disease. *Nature* 438: 960–966, 2005.
17. Garrido-Urbani S, Jemelin S, Deffert C, Carnesecchi S, Basset O, Szyndralewiez C, Heitz F, Page P, Montet X, Michalik L, Arbiser J, Ruegg C, Krause KH, and Imhof BA. Targeting vascular NADPH oxidase 1 blocks tumor angiogenesis through a PPARalpha mediated mechanism. *PLoS One* 6: e14665, 2011.
18. Gavazzi G, Banfi B, Deffert C, Fiette L, Schappi M, Herrmann F, and Krause KH. Decreased blood pressure in NOX1-deficient mice. *FEBS Lett* 580: 497–504, 2006.
19. Green DE, Murphy TC, Kang BY, Kleinhenz JM, Szyndralewiez C, Page P, Sutliff RL, and Hart CM. The Nox4 inhibitor GKT137831 attenuates hypoxia-Induced pulmonary vascular cell proliferation. *Am J Respir Cell Mol Biol* 47: 718–726, 2012.
20. Gunn DJ, Cartwright DW, and Gole GA. Incidence of retinopathy of prematurity in extremely premature infants over an 18 year period. *Clin Experiment Ophthalmol* 40: 93–99, 2011.
21. Guzik TJ, Chen W, Gongora MC, Guzik B, Lob HE, Mangalat D, Hoch N, Dikalov S, Rudzinski P, Kapelak B, Sadowski J, and Harrison DG. Calcium-dependent NOX5 nicotinamide adenine dinucleotide phosphate oxidase contributes to vascular oxidative stress in human coronary artery disease. *J Am Coll Cardiol* 52: 1803–1809, 2008.
22. Hartnett ME. The effects of oxygen stresses on the development of features of severe retinopathy of prematurity: knowledge from the 50/10 OIR model. *Doc Ophthalmol* 120: 25–39, 2010.
23. Ishida S, Yamashiro K, Usui T, Kaji Y, Ogura Y, Hida T, Honda Y, Oguchi Y, and Adamis AP. Leukocytes mediate retinal vascular remodeling during development and vaso-obliteration in disease. *Nat Med* 9: 781–788, 2003.
24. Jiang JX, Chen X, Serizawa N, Szyndralewiez C, Page P, Schroder K, Brandes RP, Devaraj S, and Torok NJ. Liver fibrosis and hepatocyte apoptosis are attenuated by GKT137831, a novel NOX4/NOX1 inhibitor *in vivo*. *Free Radic Biol Med* 53: 289–296, 2012.
25. Kim J, Kim KM, Kim CS, Sohn E, Lee YM, Jo K, and Kim JS. Puerarin inhibits the retinal pericyte apoptosis induced by advanced glycation end products *in vitro* and *in vivo* by

inhibiting NADPH oxidase-related oxidative stress. *Free Radic Biol Med* 53: 357–365, 2012.
26. Kleinschnitz C, Grund H, Wingler K, Armitage ME, Jones E, Mittal M, Barit D, Schwarz T, Geis C, Kraft P, Barthel K, Schuhmann MK, Herrmann AM, Meuth SG, Stoll G, Meurer S, Schrewe A, Becker L, Gailus-Durner V, Fuchs H, Klopstock T, de Angelis MH, Jandeleit-Dahm K, Shah AM, Weissmann N, and Schmidt HH. Post-stroke inhibition of induced NADPH oxidase type 4 prevents oxidative stress and neurodegeneration. *PLoS Biol* 8: e1000479, 2010.
27. Laleu B, Gaggini F, Orchard M, Fioraso-Cartier L, Cagnon L, Houngninou-Molango S, Gradia A, Duboux G, Merlot C, Heitz F, Szyndralewiez C, and Page P. First in class, potent, and orally bioavailable NADPH oxidase isoform 4 (Nox4) inhibitors for the treatment of idiopathic pulmonary fibrosis. *J Med Chem* 53: 7715–7730, 2010.
28. Lange C, Ehlken C, Stahl A, Martin G, Hansen L, and Agostini HT. Kinetics of retinal vaso-obliteration and neovascularisation in the oxygen-induced retinopathy (OIR) mouse model. *Graefes Arch Clin Exp Ophthalmol* 247: 1205–1211, 2009.
29. Lee J and Dammann O. Perinatal infection, inflammation, and retinopathy of prematurity. *Semin Fetal Neonatal Med* 17: 26–29, 2011.
30. McLeod DS, Brownstein R, and Lutty GA. Vaso-obliteration in the canine model of oxygen-induced retinopathy. *Invest Ophthalmol Vis Sci* 37: 300–311, 1996.
31. McLoone E, O'Keefe M, McLoone S, and Lanigan B. Long term functional and structural outcomes of laser therapy for retinopathy of prematurity. *Br J Ophthalmol* 90: 754–759, 2006.
32. Miyamoto K, Khosrof S, Bursell SE, Rohan R, Murata T, Clermont AC, Aiello LP, Ogura Y, and Adamis AP. Prevention of leukostasis and vascular leakage in streptozotocin-induced diabetic retinopathy *via* intercellular adhesion molecule-1 inhibition. *Proc Natl Acad Sci USA* 96: 10836–10841, 1999.
33. Moravski CJ, Kelly DJ, Cooper ME, Gilbert RE, Bertram JF, Shahinfar S, Skinner SL, and Wilkinson-Berka JL. Retinal neovascularization is prevented by blockade of the renin-angiotensin system. *Hypertension* 36: 1099–1104, 2000.
34. Mowat FM, Luhmann UF, Smith AJ, Lange C, Duran Y, Harten S, Shukla D, Maxwell PH, Ali RR, and Bainbridge JW. HIF-1alpha and HIF-2alpha are differentially activated in distinct cell populations in retinal ischaemia. *PLoS One* 5: e11103, 2010.
35. Nielsen JC, Naash MI, and Anderson RE. The regional distribution of vitamins E and C in mature and premature human retinas. *Invest Ophthalmol Vis Sci* 29: 22–26, 1988.
36. Niesman MR, Johnson KA, and Penn JS. Therapeutic effect of liposomal superoxide dismutase in an animal model of retinopathy of prematurity. *Neurochem Res* 22: 597–605, 1997.
37. Oliner JD, Bready J, Nguyen L, Estrada J, Hurh E, Ma H, Pretorius J, Fanslow W, Nork TM, Leedle RA, Kaufman S, and Coxon A. AMG 386, a selective angiopoietin 1/2-neutralizing peptibody, inhibits angiogenesis in models of ocular neovascular diseases. *Invest Ophthalmol Vis Sci* 53: 2170–2180, 2012.
38. Park K, Jin J, Hu Y, Zhou K, and Ma JX. Overexpression of pigment epithelium-derived factor inhibits retinal inflammation and neovascularization. *Am J Pathol* 178: 688–698, 2011.
39. Penn JS, Tolman BL, and Bullard LE. Effect of a water-soluble vitamin E analog, trolox C, on retinal vascular development in an animal model of retinopathy of prematurity. *Free Radic Biol Med* 22: 977–984, 1997.
40. Pierce EA, Foley ED, and Smith LE. Regulation of vascular endothelial growth factor by oxygen in a model of retinopathy of prematurity. *Arch Ophthalmol* 114: 1219–1228, 1996.
41. Pizzolla A, Hultqvist M, Nilson B, Grimm MJ, Eneljung T, Jonsson IM, Verdrengh M, Kelkka T, Gjertsson I, Segal BH, and Holmdahl R. Reactive oxygen species produced by the NADPH oxidase 2 complex in monocytes protect mice from bacterial infections. *J Immunol* 188: 5003–5011, 2012.
42. Raju TN, Langenberg P, Bhutani V, and Quinn GE. Vitamin E prophylaxis to reduce retinopathy of prematurity: a reappraisal of published trials. *J Pediatr* 131: 844–850, 1997.
43. Ritter MR, Banin E, Moreno SK, Aguilar E, Dorrell MI, and Friedlander M. Myeloid progenitors differentiate into microglia and promote vascular repair in a model of ischemic retinopathy. *J Clin Invest* 116: 3266–3276, 2006.
44. Saito Y, Geisen P, Uppal A, and Hartnett ME. Inhibition of NAD(P)H oxidase reduces apoptosis and avascular retina in an animal model of retinopathy of prematurity. *Mol Vis* 13: 840–853, 2007.
45. Sapieha P, Joyal JS, Rivera JC, Kermorvant-Duchemin E, Sennlaub F, Hardy P, Lachapelle P, and Chemtob S. Retinopathy of prematurity: understanding ischemic retinal vasculopathies at an extreme of life. *J Clin Invest* 120: 3022–3032, 2010.
46. Sasaki M, Ozawa Y, Kurihara T, Kubota S, Yuki K, Noda K, Kobayashi S, Ishida S, and Tsubota K. Neurodegenerative influence of oxidative stress in the retina of a murine model of diabetes. *Diabetologia* 53: 971–979, 2010.
47. Schroder K, Zhang M, Benkhoff S, Mieth A, Pliquett R, Kosowski J, Kruse C, Ludike P, Michaelis UR, Weissmann N, Dimmeler S, Shah AM, and Brandes RP. Nox4 Is a protective reactive oxygen species generating vascular NADPH oxidase. *Circ Res* 110: 1217–1225, 2012.
48. Segal BH, Leto TL, Gallin JI, Malech HL, and Holland SM. Genetic, biochemical, and clinical features of chronic granulomatous disease. *Medicine (Baltimore)* 79: 170–200, 2000.
49. Selemidis S, Sobey CG, Wingler K, Schmidt HH, and Drummond GR. NADPH oxidases in the vasculature: molecular features, roles in disease and pharmacological inhibition. *Pharmacol Ther* 120: 254–291, 2008.
50. Sivakumar V, Foulds WS, Luu CD, Ling EA, and Kaur C. Retinal ganglion cell death is induced by microglia derived pro-inflammatory cytokines in the hypoxic neonatal retina. *J Pathol* 224: 245–260, 2011.
51. Stahl A and Smith LE. An eye for discovery. *J Clin Invest* 120: 3008–3011, 2010.
52. Stone J, Chan-Ling T, Pe'er J, Itin A, Gnessin H, and Keshet E. Roles of vascular endothelial growth factor and astrocyte degeneration in the genesis of retinopathy of prematurity. *Invest Ophthalmol Vis Sci* 37: 290–299, 1996.
53. Tan SM, Stefanovic N, Tan G, Wilkinson-Berka JL, and de Haan JB. Lack of the antioxidant glutathione peroxidase-1 (GPx1) exacerbates retinopathy of prematurity in mice. *Invest Ophthalmol Vis Sci* 54: 555–562, 2013.
54. Ushio-Fukai M, Tang Y, Fukai T, Dikalov SI, Ma Y, Fujimoto M, Quinn MT, Pagano PJ, Johnson C, and Alexander RW. Novel role of gp91(phox)-containing NAD(P)H oxidase in vascular endothelial growth factor-induced signaling and angiogenesis. *Circ Res* 91: 1160–1167, 2002.
55. Wang AL, Yu AC, He QH, Zhu X, and Tso MO. AGEs mediated expression and secretion of TNF alpha in rat retinal microglia. *Exp Eye Res* 84: 905–913, 2007.

56. Wilkinson-Berka JL, Rana I, Armani R, and Agrotis A. Reactive oxygen species, Nox and angiotensin II in angiogenesis: implications for retinopathy. *Clin Sci (Lond)* 124: 597–615, 2013.
57. Wilkinson-Berka JL, Tan G, Binger KJ, Sutton L, McMaster K, Deliyanti D, Perera G, Campbell DJ, and Miller AG. Aliskiren reduces vascular pathology in diabetic retinopathy and oxygen-induced retinopathy in the transgenic (mRen-2)27 rat. *Diabetologia* 54: 2724–2735, 2011.
58. Wilkinson-Berka JL, Tan G, Jaworski K, and Miller AG. Identification of a retinal aldosterone system and the protective effects of mineralocorticoid receptor antagonism on retinal vascular pathology. *Circ Res* 104: 124–133, 2009.
59. Wingler K, Hermans JJ, Schiffers P, Moens A, Paul M, and Schmidt HH. NOX1, 2, 4, 5: counting out oxidative stress. *Br J Pharmacol* 164: 866–883, 2011.
60. World Health Organization. Global initiative for the elimination of avoidable blindness: action Plan 2006–2011. Geneva: World Health Organization; 2007. Available from: www.who.int/blindness/Vision2020_report.pdf (accessed July 4 2012), 2007.
61. Yoshida S, Yoshida A, Ishibashi T, Elner SG, and Elner VM. Role of MCP-1 and MIP-1alpha in retinal neovascularization during postischemic inflammation in a mouse model of retinal neovascularization. *J Leukoc Biol* 73: 137–144, 2003.
62. Zhang M, Brewer AC, Schroder K, Santos CX, Grieve DJ, Wang M, Anilkumar N, Yu B, Dong X, Walker SJ, Brandes RP, and Shah AM. NADPH oxidase-4 mediates protection against chronic load-induced stress in mouse hearts by enhancing angiogenesis. *Proc Natl Acad Sci USA* 107: 18121–18126, 2010.

Address correspondence to:
Prof. Jennifer L. Wilkinson-Berka
Department of Immunology
Monash University
Level 5, Alfred Centre
Alfred Medical Research and Education Precinct (AMREP)
99 Commercial Road
Melbourne 3004
Australia

E-mail: jennifer.wilkinson-berka@monash.edu

Date of first submission to ARS Central, April 14, 2013; date of final revised submission, September 7, 2013; date of acceptance, September 22, 2013.

Abbreviations Used

DHE = dihydroethidium
EPO = erythropoietin
HBSS = Hank's balanced salt solution
Iba1 = ionizing binding adaptor molecule-1
ICAM-1 = intercellular adhesion molecule-1
KO = knockout
NOX = NADPH oxidase
OIR = oxygen-induced retinopathy
PBS = phosphate-buffered saline
PCR = polymerase chain reaction
P = postnatal day
ROS = reactive oxygen species
VEGF = vascular endothelial growth factor